J. Biomater. Sci. Polymer Edn, Vol. 15, No. 10, pp. 1263–1280 (2004)

Also available online - www.vsppub.com

Changes in morphology of starch-based prothestic thermoplastic material during enzymatic degradation

M. ALBERTA ARAÚJO [1,2,3,*], ANTÓNIO M. CUNHA [3] and MANUEL MOTA [1]

[1] *Centro de Engenharia Biológica, University of Minho, Campus de Gualtar, 4710-057 Braga, Portugal*
[2] *Escola Superior de Tecnologia e Gestão, IPVC, Avenida Atlântico, 4900 Viana do Castelo, Portugal*
[3] *Department of Polymer Engineering, University of Minho, Campus de Azurém, 4800-058 Guimarães, Portugal*

Received 21 October 2003; accepted 17 February 2004

Abstract—This work evaluates the structural changes of an interpenetrated starch thermoplastic blend withstanding different enzymatic α-amylase degradation periods (up to 200 days), and establishes the relationships between the kinetics degradation rate and the structure of the material. It characterises the different stages of the enzymatic degradation process on starch/ethylenevinyl-alcohol blends, based on the attack of the connected starch domains that can be accessed by the enzymatic solution. The completely encapsulated starch particles remain practically unchanged. Furthermore, it was also found that the enzymatic degradation process was limited after 100 days of immersion. In order to understand such phenomenon several techniques were used, namely differential scanning calorimetry, contact-angle measurements, high-performance liquid chromatography, Fourier transform infrared spectrometry, scanning electron microscopy and atomic force microscopy. The materials were evaluated with respect to the enzymatic degradation rate, surface morphology and degradation behaviour. The results show that the ethylene-vinylalcohol phase wraps the starch domains, preventing the respective degradation. Consequently, the degraded material in the solution comes only from the starch particles that could be reached by the enzyme.

Key words: Biodegradable polymer; porosity; starch; enzyme; surface analysis; microstructure.

INTRODUCTION

Different starch/synthetic polymer blends have been suggested to have potential for use in distinct biomedical applications [1, 2].

*To whom correspondence should be addressed at the Centro de Engenharia Biológica. Tel.: (351-253) 604-400. Fax: (351-253) 678-986. E-mail: alberta@deb.uminho.pt

The chemical and the physical properties of starch have been widely investigated due to its suitability to be converted into a thermoplastic and to be used in different applications as a result of its known biodegradability, availability and economical competitiveness [3, 4]. Furthermore, it has been shown in several studies that these polymeric systems exhibit appropriate degradation kinetics [5–7] and biocompatible behaviour [8, 9].

Structure of thermoplastic starch-based blends

The structure at the molecular level of starch-based blends is complex, involving interpenetrated networks and other physical and chemical interactions [10].

The starch and the ethylene-vinylalcohol (EVOH) are combined into an interpenetrated network forming droplet-like microstructures [11]. In fact, different microstructures were observed in starch/vinyl-alcohol copolymers [12], from droplet to layer-like morphologies, depending on the different hydrophilicity of the synthetic copolymer [13].

The final blend morphology depends upon the processing conditions used and will influence the mechanical properties and the degradation modes of the respective products. For example, crystallinity will decrease the degradation rate and will contribute to inhibit the accessibility to the bulk zones of the blends [14].

Degradation of starch-based blends

Polymer degradation has a major importance in the production, and use of implantable and other medical devices as an ideal material to be used in temporary bone replacement should associate an adequate range of mechanical properties (matching those of bone), with convenient degradation kinetics, a bone-bonding behaviour and a biocompatible performance [15].

Several researchers have underlined the role of enzymes, free radicals and phagocytic cells in the process and biodegradable polymers [16–20]. However, there is no clear pattern of the respective mechanisms and, consequently, there are no general procedures for predicting, preventing and controlling this type of degradation.

This paper addresses the enzymatic and morphological different stages and mechanisms involved in the complex degradation processes of these blends, based on the obtained experimental results. Attention is also given to the role of microstructure in determining the biodegradation rate of this class of products.

In a previous work [1] we speculated that EVOH chains were responsible for the residual non-degraded starch and for the degradation limitation observed after 100 days of immersion.

In order to prove this assumption, several techniques were used, such as differential scanning calorimetry (DSC), contact-angle measurements, high-performance liquid chromatography (HPLC), Fourier transform infrared spectrometry (FT-IR), scanning electron microscopy (SEM) and atomic force microscopy (AFM).

MATERIALS AND METHODS

Materials

The material studied was a thermoplastic blend of corn starch with a poly(ethylene-vinyl alcohol) copolymer (60 : 40, mol/mol), SEVA-C, supplied by Novamont (Italy). The typical amount of starch in this commercially available blend is 50–60 wt%. Two different specimens were used: injection moulded square plates (30 mm wide and 2 mm thickness) and cylindrical rods (10 mm diameter and thickness 1 mm).

The SEVA-C samples were weighed and immersed for several pre-fixed ageing periods as long as 6 months, at pH 7.4 and 37 ± 1 °C in individual containers (volume approximately 50 cm^3) with Hank's balanced salt solution (HBSS) without phenol red (HBSS Sigma reference H8264), with α-amylase (from human saliva, Sigma reference A0521) with different concentrations (50, 100 and 150 units/l). The enzyme solution had an activity of 0.35 mg/unit per min at pH 6.9 and 20°C per gram of soluble starch. To stabilise α-amylase, 1 mM calcium chloride was employed.

The square plates were used in *in vitro* degradation experiments under controlled conditions inside a laminar flux chamber. The cylindrical specimens were used to study the surface morphology using SEM and AFM.

All the samples were sterilized by autoclave in an atmosphere consisting of a 10 : 90 mixture of ethylene oxide (EtO) and carbon dioxide (CO_2), with a cycle time of 20–22 h at a working temperature of 45 °C and a chamber pressure of 180 kPa.

Enzymatic methods

Determination of kinetic values for α-amylase. The kinetic values (K_m and v_{max}) for α-amylase were found using the Eadie–Hoffstee method, for different starch solutions [21]. In order to calculate these kinetic values at the conditions of the degradation process, an α-amylase concentration of 50 units/l was selected (the same concentration was used for SEVA-C specimen degradation trials). Three trials were performed, considering the average of all results as the final values of K_m and v_{max}.

Five buffered (pH 7.0) aqueous starch solutions (50 ml) of 0.5%, 1%, 1.5%, 2% and 2.5% (w/v) were prepared. The procedure included the following stages: (i) heating under continuous stirring until boiling, (ii) cooling of the obtained gelatinised starch solution to room temperature and (iii) heating to the stabilizing temperature of 37°C. The enzymatic digestion process was started by adding 20 μl of enzyme to 10 ml of each shacked and mixed starch solution. The hydrolysis proceeded for 250 min at 37°C and samples were periodically taken (each 10 min) to monitor the increase of reducing sugars, until most of the starch was hydrolysed. The increased sugar concentration was followed with the dinitrosalicylic colorimetric method (DNS) [22]. After measuring the soluble reducing sugars, the reaction rate was calculated for each substrate concentration.

Plots of S/v *versus* v gave straight lines (where v and S are the velocity and substrate concentration, respectively). The kinetic parameters (K_m and v_{max}) were obtained from the slope and the intercepts of these straight line plots, expressed as g/l and g/l per min, respectively.

Determination of the initial enzyme activity. The initial activity exhibited by the enzyme purchased was quantified using three enzyme concentrations: 50, 100 and 150 unit/l.

These experiments enabled to evaluate whether the enzyme was active initially and the activity loss with time.

Starch (1%) was dissolved in a phosphate buffer solution (pH 7.0). Then, α-amylase was added to starch solution, to obtain 50, 100 and 150 units/l of enzyme concentrations. The hydrolysis proceeded following the method described above.

The activity was evaluated for each enzyme concentration, expressed as mg glucose/unit/min at the first stages of reaction.

Evolution of the enzyme activity along the degradation trials. The enzyme activity was followed during the degradation trials, in order to evaluate any deactivation throughout the assays. Three enzyme concentrations were studied: 50, 100 and 150 unit/l, to analyse the differences in the enzyme activity. The three solutions were dissolved in HBSS at pH 7.4 and 37°C, and kept in these conditions during a period similar to the degradation assays.

At pre-defined periods, once a week, 0.5 ml of each enzyme solution was added to 0.5 ml of 1% buffered starch solution (pH 7.0) and incubated at 37°C during 20 min, to monitor the enzymatic activation/deactivation process. After incubation, the reaction was stopped by adding 1 ml DNS to 1 ml of the mixture.

The enzyme activity was expressed as mg glucose/unit per min for each enzyme concentration and as a function of the immersion time. Each value represents the mean of 2 duplicates from 3 enzyme concentrations (4 values in all). Error bars using Student's t-test were plotted along with mean values based on 95% confidence intervals.

Mass of saccharides released for different enzyme concentrations. The structural limitation of SEVA-C to α-amylase degradation (penetration) was evaluated. As before, the same three enzyme concentrations were used, compared with the one used in the degradation trials (50 units/l), and dissolved in HBSS until approximately 150 days. The increased sugar concentration was followed twice a week using the DNS method. HBSS and SEVA-C specimens without enzymes were used for control purposes.

The mass of glucose released in the solution was obtained for each enzyme concentration per specimen mass. Each value represents the mean of 2 duplicates from 3 enzyme concentrations (4 values in total). Error bars using Student's t-test were plotted along with mean values based on 95% confidence intervals.

Interactions between oligosaccharides and glycerol in the enzymatic solutions. To evaluate any side-effects and changes that might occur between oligosaccharides and glycerol in α-amylase solutions, the compounds were mixed together and the respective products were analysed by HPLC as a function of immersion time. HPLC with 830-RI (Jasco, Japan) refraction index detection and a 880-PU pump (Jasco) was used to separate the sugar derivatives and glycerol of the solutions.

Commercial standards were used for the calibration of the Chrompack carbohydrates Ca column. A Chrompack guard column at 90°C with ultra-pure water as eluent (0.5 ml/min), was maintained at a pressure 6500–7000 kPa. The eluent was filtered through a 0.2 μm sterilized membrane degassed with helium prior to be used, and kept in a container that precludes introduction of airborne bacterial and fungal contamination. Sorbitol (1 g/l) was used as the internal standard. Prior to the injection the samples were filtered through 0.22 mm filters (Millipore) to remove the particles present in the degradation solutions. A standard curve was previously built using different standard concentrations. Maltose (1.5 g/l), glucose (3 g/l) and glycerol (1 g/l) were dissolved separately on HBSS with 50 units/l of α-amylase at 37°C and pH 7.4. Another assay was performed with the same compounds (1 g/l) mixed together with α-amylase during 150 days of immersion. Samples of each solution were taken every week and the sugar derivatives and glycerol were analysed by HPLC.

Morphological methods

Contact angle measurements and surface free energy determinations. The effect of the enzyme degradation on the surface free energy of SEVA-C specimens, as a function of the immersion time, was followed by contact angle measurements. The plates were dried at 80°C for 1 week and kept in a desiccator. These measurements were carried out at room temperature, in a standard contact angle apparatus (Kruss), using the sessile-drop technique, with a video camera mounted on a microscope to record the drop image. Sessile drops were deposited with a micrometric syringe directly on the surface from the metallic needle. Pictures of the drops were taken in manual mode at regular intervals, in order to avoid errors of the automatic baseline.

Surface free energy and surface tension components were calculated by using the Van Oss method [23]. The probe liquids for surface free energy components determinations were water, diiodomethane and formamide. The surface free energy parameters of these liquids are listed in Table 1.

Table 1.
Surface tension parameters of probe liquids [2] in mJ/m^2

Liquid	γ^{TOT}	γ^{LW}	γ^+	γ^-
Water	72.8	21.8	25.5	25.5
Diiodomethane	50.8	50.8	0	0
Formamide	58.0	39.0	2.3	39.6

At least 30 measurements using drops of about 6 μl for each liquid were performed for each sample analysed.

Differential scanning calorimetry. DSC was performed in a Shimadzu DSC-50 calorimeter using aluminium pans, under the following conditions: heating rate 5°C/min, target temperature 200°C, under a constant helium flow of 30 ml/min. An aluminium crucible covered with a lid and crimped without anything therein was used as reference material on the left side of the detector plate.

The pre-conditioning was as follows: samples of about 10 mg were removed for testing at a pre-defined immersion time (for 200 days) and kept in a desiccator with controlled temperature and humidity. The equilibrium hydration degree was considered attained when no weight change (0.01 g) was observed. For control, a non-immersed specimen, stored at controlled environment conditions. The assays were performed in six different samples, considering the average of all the results as the final value. Two determinations were performed: peak temperature and heat flux on automatic exo/endothermic peak analysis. The enthalpy (J/g) was calculated accordingly to the samples weight before the analysis.

Fourier transform infrared spectrometry. FT-IR was selected to assess possible changes in the chemical structure of the polymeric chains, which might have been induced by processing. It has been reported [2] that starch-based polymers are very sensitive to thermal degradation during melt processing. Consequently, two different materials were evaluated, SEVA-C and starch. Starch was analysed after boiling in distilled water, under stirring for 5 h and compared with the non-treated samples. The samples were freeze dried in a Freeze Dryer Alpha 2-4 and the resulting powders were conditioned in a desiccator prior to FT-IR analysis. FT-IR spectra were recorded using a Perkin Elmer 1600 spectrophotometer with an attenuated total reflectance (ATR) device, with a resolution of 2 cm^{-1} and averaged over 16 scans.

In order to get a better resolution of the overlapping peaks the second derivative of FT-IR spectra was used. The analysis was also performed in the field of the starch ring vibrations between 960 and 920 cm^{-1}, to assess the starch type.

Scanning electron microscopy. The possible changes on the surface morphology of SEVA-C in contact with enzymatic solution, as a function of immersion time, were followed by SEM using a Leica Cambridge S360 microscope. The plates were dried at 80°C for 1 week and the surface was cleaned and kept in a desiccator before analysis. For control, a non-immersed specimen, stored under controlled environment conditions, was used.

The microstructure was also studied on samples obtained after boiling approximately 0.2 g of SEVA-C (square plates and powder) and starch in 150 ml of distilled water, under stirring for 5 h. SEVA-C powder was used for the analysis, since it was more easily dissolved. The samples were freeze dried in a Freeze Dryer Alpha 2-4. The resulting powders were conditioned in a desiccator prior to SEM analysis.

Atomic force microscopy. To observe the surface and roughness properties of SEVA-C specimens, as a function of the immersion time, a NanoScope III atomic force microscope was used (Digital Instruments).

Cylindrical specimens of 10 mm diameter and thickness 1 mm were used. Before analysis, the specimens were cleaned ultrasonically in acetone, rinsed with distilled water, and stored in desiccators under constant relative humidity.

The *in situ* observation was performed in tapping mode. The lateral scanning movement of the tip occurs above the surface so that it only touches the surface for a very small fraction of its oscillation. A silicon tip was used. All the images were recorded with a scan size of 10×10 μm and a data scale of 1500 nm.

The surface roughness of the specimens was measured, as a function of the immersion time, using the software installed in the AFM. The common measurements of roughness were used: RMS (root mean square), R_a (mean roughness) and R_{max} (maximum roughness).

RESULTS AND DISCUSSION

Evaluation of the enzymatic activity

Kinetic values of α-amylase. As α-amylase was used to promote the degradation of SEVA-C material, the main properties of this enzyme at the conditions of the assay were carefully assessed. The obtained kinetic values (K_m and v_{max}) are presented in Table 2.

The v_{max} found (12.2 mg/l min) is much higher than the one obtained for the degradation of polysaccharides with the same enzyme concentration (0.045 mg/l min [1]). In fact, the conditions are quite different in the two cases. In the first case, starch was dissolved and therefore freely accessible to the enzyme molecules, whereas in the second case starch phase was encapsulated and strongly interpenetrated inside the synthetic component of the blend, hindering the access of the enzyme.

Enzyme activity. The enzyme activity was evaluated for three different concentrations (the activity referred to by the supplier was 0.35 mg glucose/unit per min at 20°C and pH 6.9). The values found were around 0.095 mg glucose/unit per min, corresponding to 27% of the theoretical enzyme activity.

Table 2.
Kinetic parameters, K_m and v_{max}, for three assays performed

Assay	v_{max} (mg/l per min)	K_m (g/l)
1	15.2	1.01
2	11.5	1.71
3	12.2	1.51
Average	12.2 ± 3	1.5 ± 0.5

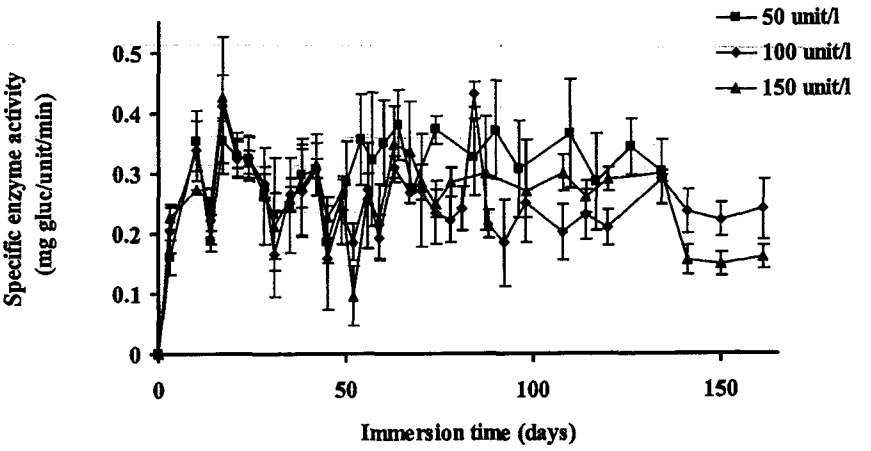

Figure 1. Enzyme activity (in mg glucose/unit per min) for three enzyme concentrations 50, 100 and 150 units/l, as function of immersion time. Each value represents the mean of 2 duplicates (4 values in all); error bars are 95% confidence intervals of each mean.

The purpose was to analyse any deactivation/activation process or ageing that may occur during the enzymatic degradation of SEVA-C (Fig. 1). A mean value of 0.3 mg glucose/unit per min was obtained (around 86% of the reference activity).

Despite the smaller enzyme activity, there was no deactivation along the assay. As expected, the enzyme activity was similar for the 3 enzyme concentrations throughout the assay, no significant differences were observed between these 3 concentrations, as was validated by applying Student's t-test to the experimental results. Values are the same at the 95% confidence interval.

Mass of saccharides released for different enzyme concentrations. The kinetics of the enzymatic reaction may be described by a linear correlation between the hydrolysis rate and the substrate concentration (first-order reaction), followed by a second stage corresponding to enzyme saturation (zero-order reaction) [21].

Figure 2 shows the increased reducing sugars released per specimen mass, as a function of immersion time and enzyme concentration. The glucose release follows a similar trend for the different enzyme concentrations, increasing rapidly in a first stage (80 days) tending towards a level around 19%. As the enzyme concentration rises, the SEVA-C surface becomes completely coated with enzyme and the reaction rate becomes proportional to the concentration of reactive sites (effective concentration). From 80 days on, the level of released glucose tends to stabilize as was validated by applying Student's t-test to the experimental results, probably because the available sites for enzyme degradation decrease, no significant differences were observed between these three concentrations. Values are the same at the 95% confidence interval.

These results lead to the conclusion that even 50 units/ml becomes a saturating enzyme concentration after day 80.

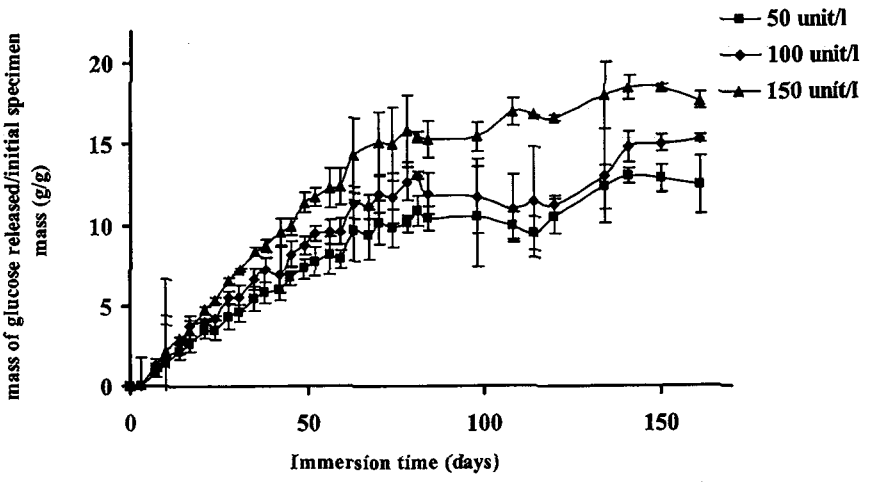

Figure 2. Mass of glucose released to the solution for each enzyme concentration, 50, 100 and 150 unit/l, per initial specimen mass (1.61 g) in 50 ml of solution, as a function of immersion time. Each value represents the mean of 2 duplicates (4 values in all); error bars are 95% confidence intervals of each mean.

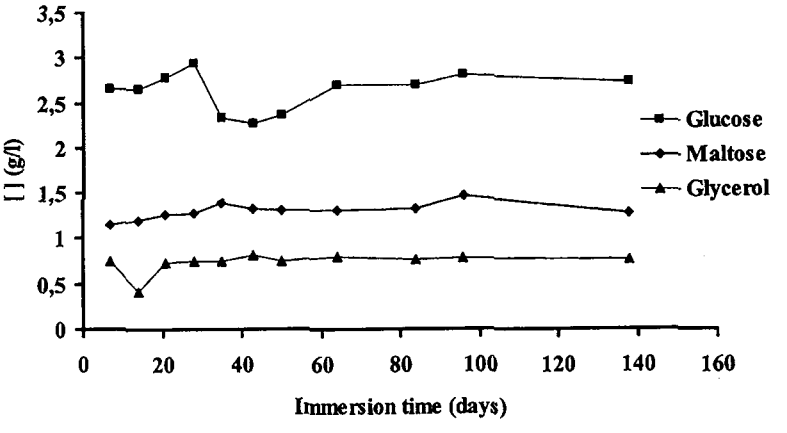

Figure 3. Glucose, maltose and glycerol concentrations as a function of immersion time.

Interactions between oligosaccharides and glycerol. Figure 3 shows the evolution of the glucose, maltose and glycerol concentrations in the enzymatic simulated solution as a function of immersion time (for the case of mixed compounds). No interaction between the saccharides and glycerol, and between them and the enzyme, was observed. In fact, the respective concentrations remain almost invariable during the 150 days of the assay (Fig. 4). Similar results were obtained for the study with the compounds isolated.

Surface morphology of SEVA-C

Contact-angle measurements and surface free energy. The contact-angle measurements for SEVA-C surface treated with and without enzymes as a function of

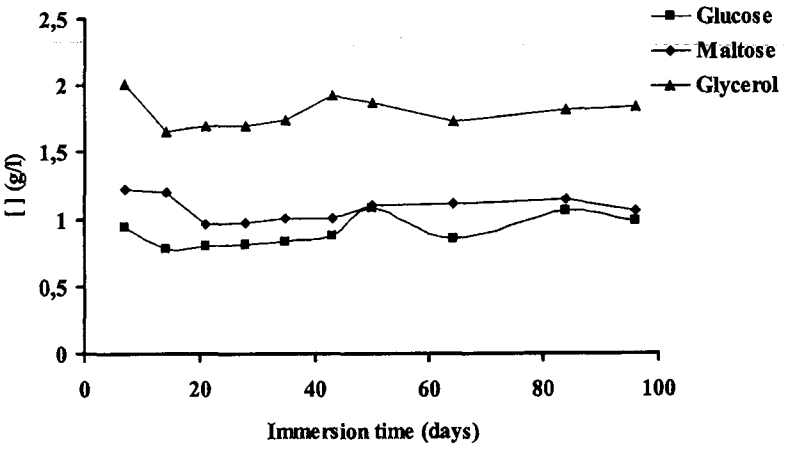

Figure 4. Glucose, maltose and glycerol concentrations (mixed together) as a function of immersion time.

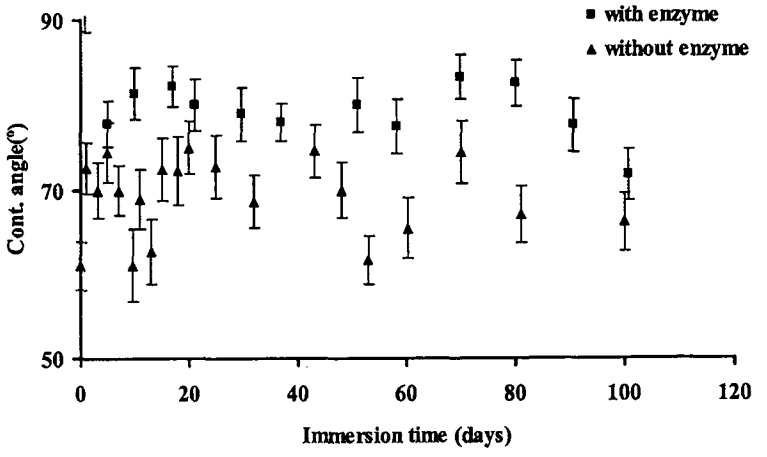

Figure 5. Contact-angle measurements for water on SEVA-C, treated with and without enzymes, as a function of immersion time (measurements in dried samples).

immersion time are summarized in Fig. 5. As in both cases the contact angle was higher than 50°, SEVA-C surface was considered as hydrophobic.

The two cases exhibit an almost negligible variation with the immersion time and a small difference between them. However, the enzymatically-degraded surfaces exhibit a higher hydrophobicity, since the average contact angles are systematically higher than the ones obtained without enzyme. This result should be the combined effect of the following features: higher surface roughness, less amorphous starch available on the outer surface, increased porosity (confirmed by SEM and AFM results) and lower water content.

The surface free energy of enzyme treated SEVA-C (Table 3) revealed that the apolar component ($\gamma^{LW} = 24$ mJ/m^2) remains constant during the immersion

Table 3.
Surface tension components of SEVA-C surface (in mJ/m^2), determined by contact angle measurements, for different immersion times

Immersion time (days)	γ_s^{LW}	γ_s^-	γ_s^+	γ_s^{AB}	γ_s^{TOT}
5	22.02	14.19	0.39	4.7	26.72
37	26.62	13.69	0.55	5.5	32.17
80	22.07	6.46	1.29	5.78	27.85
101	23.89	12.33	0.4	4.43	28.32

Table 4.
Interfacial free energy of interaction (ΔG_{sws}, in mJ/m^2) between the surface (s) and water (w), calculated from the surface free energy components listed in Table 1, for different immersion times

Immersion time (days)	ΔG_{sws}^{LW}	ΔG_{sws}^{AB}	ΔG_{sws}^{TOT}
5	−0.001	−22.71	−22.71
37	−0.48	−23.25	−23.73
80	−0.002	−39.26	−39.26
101	−0.096	−27.19	−27.29

time, being predominantly electron donating ($\gamma_s^- > \gamma_s^+$) and hydrophobic ($\gamma_s^- < 28\ mJ/m^2$).

The values of the free energy of the hydrophobic interaction are in the same magnitude (Table 4), confirming a negligible variation with the immersion time. These values also evidence the surface hydrophobic nature ($\Delta G_{sup}^{TOT} < 0$).

DSC. DSC analyses were carried to evaluate eventual changes on the semicrystalline structure of SEVA-C during the degradation process.

Typical thermograms for increasing immersion times are shown in Fig. 6. It is clear that the temperature of the EVOH fusion peak (around 140°C) remains almost constant and the magnitude of the starch endotherm is reduced along the time.

Figure 7 presents the enthalpy variation of the EVOH fusion with the immersion time.

Both results sustain the idea of a preferential attack of the amorphous phase during the degradation process.

SEM. Figure 8 shows SEM micrographs of SEVA-C material, before and after 200 degradation days in HBSS with enzymatic activity.

The increase in the surface porosity as a function of immersion time can be seen clearly. Note that the control sample (Fig. 8a) has a smooth surface compared to the very rough degradation sample (Fig. 8d). This phenomenon should be related to a hydrolytic surface dissolution of the original sample.

The porous average size ranges from 300 to 400 nm.

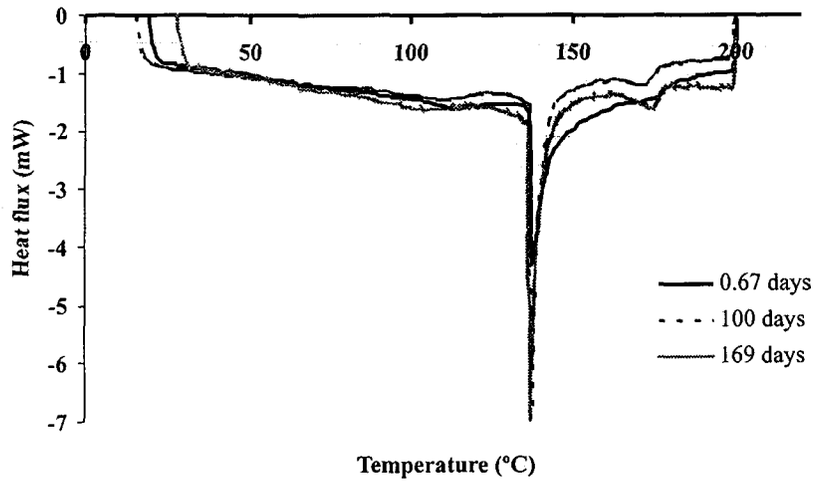

Figure 6. DSC thermograms for SEVA-C after 0.67, 100 and 169 immersion days.

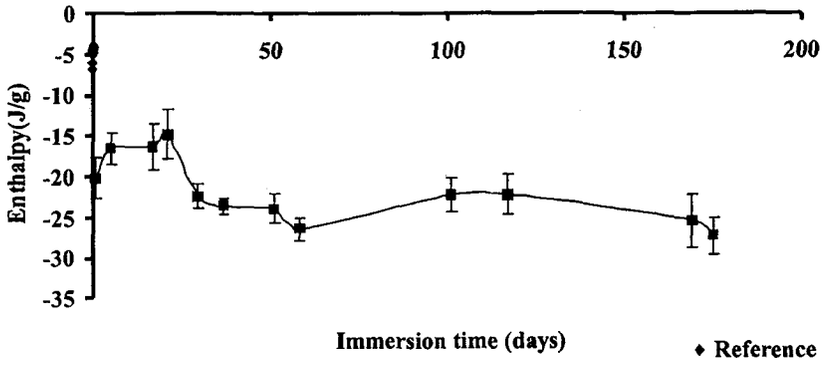

Figure 7. Enthalpy associated to SEVA-C degradation *versus* immersion time (data obtained from DSC analysis).

The microstructure of boiled SEVA-C and starch was also observed with SEM. Under these conditions the EVOH/starch materials did not dissolve, forming a micro dispersion constituted by microsphere aggregates. The microspheres observed had a droplet-like structure (Fig. 9). The droplet size is comparable with that of the microdispersion obtained, due to the ability of starch to generate hydrophobic interactions with ethylene vinylalcohol copolymers (EVOH).

As demonstrated by previous results [1], for longer immersion times, as high as 100 days, the degradation rate tends to stabilize, although the enzyme is still active. A possible hypothesis to explain this behaviour could be the increased difficulty for enzymes to reach starch molecules strongly interspersed in the synthetic, insoluble component in the droplet-like structure.

The residual starch that remains in the structure, after a long degradation period, is surrounded by non-degraded EVOH chains, that form a barrier to further

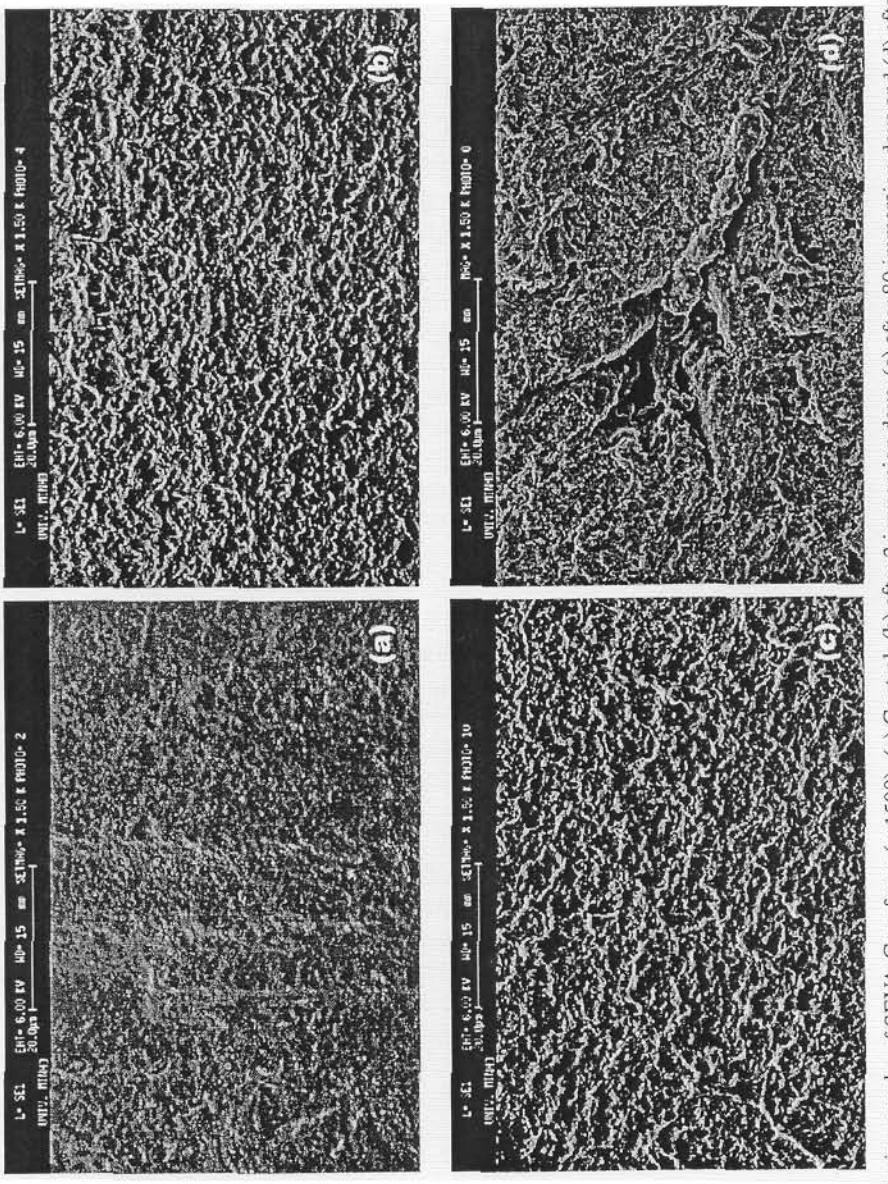

Figure 8. SEM micrographs of SEVA-C surfaces (×1500). (a) Control, (b) after 3 immersion days, (c) after 80 immersion days and (d) after 117 immersion days. The images present dried samples after the immersion time.

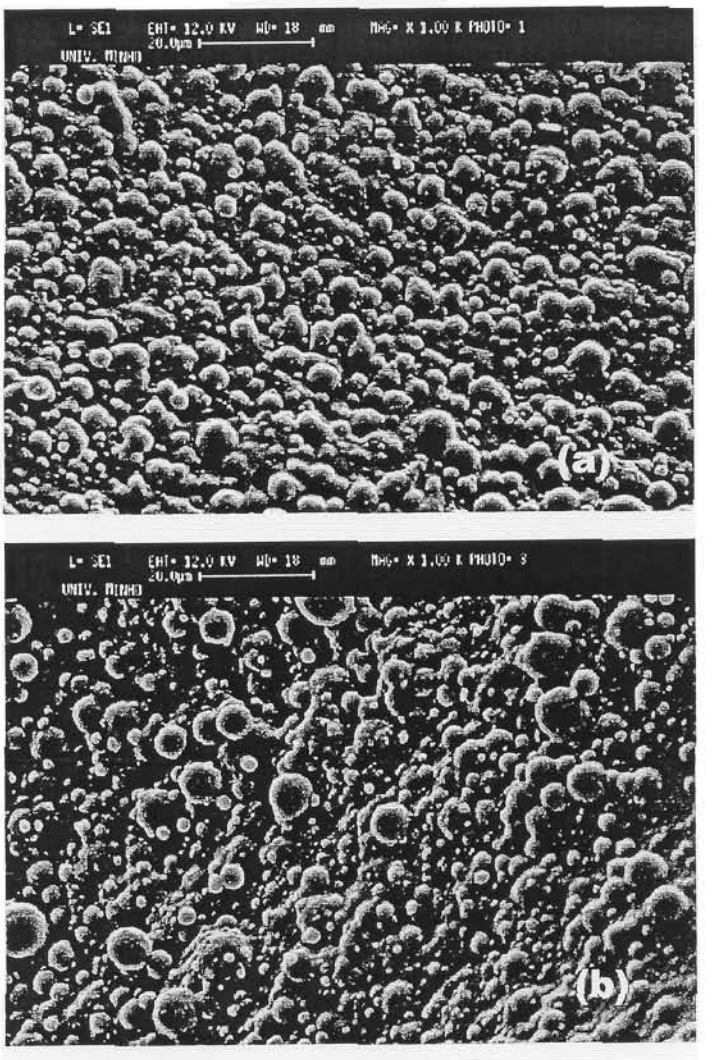

Figure 9. SEM micrographs of SEVA-C surfaces. (a) Square plate and (b) powder after desegregation in boiling distilled water for 5 h (×1000). The images present freeze-dried samples after boiling.

degradation. Figure 9a and 9b shows SEVA-C structure after boiling in water and it seems that the continuous starch form complexes in the presence of EVOH, generating a granular shape.

These images support the idea of a degradation mechanism based on the enzymatic activity on the material surface and interconnected starch zones and inhibited in the zones where the EVOH copolymer wraps the starch domains.

As compared with SEVA-C, the micrographs showing the morphology of a pure starch plate after boiling (Fig. 10) exhibited a smooth surface, with few voids that result from degradation.

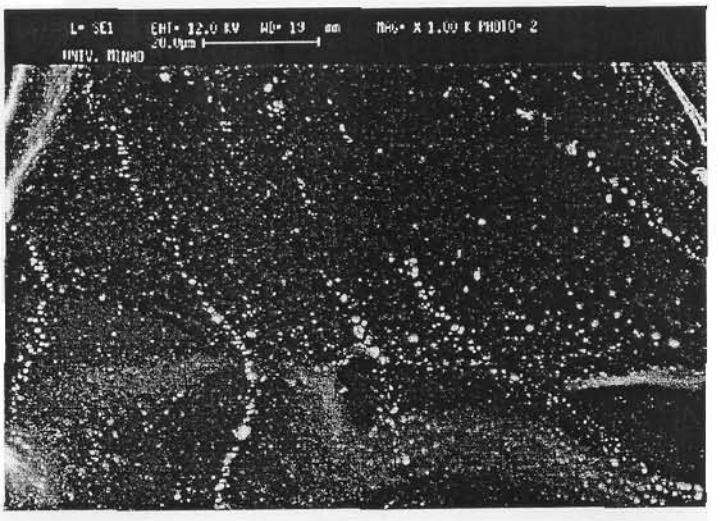

Figure 10. SEM micrograph of starch surfaces (square plate) after desegregation in boiling distilled water for 5 h (×1000). The image presents a freeze-dried sample after boiling.

Table 5.
Surface roughness of SEVA-C specimens in RMS (root mean square), R_a (mean roughness) and R_{max} (maximum roughness) for different immersion times

Immersion time (days)	R_a (*nm*)	RMS (*nm*)	R_{max} (μm)
Control	47.21	63.19	0.66
21	169.98	218.97	1.43
91	184.13	242.78	2.53
101	384.17	497.74	2.98

AFM. The AFM tapping mode topographic images confirm the increased porosity as a function of immersion time (Fig. 11). Small protrusions were observed at the surface of the blends. The specimen with a longer immersion time (102 days) showed structural voids and crevices. As the roughness increased for specimens with longer immersion time, the specific area available for degradation became enlarged.

The mean roughness goes from 47.2 nm for control to 384.2 nm for specimens with longer immersion time (102 days). The same behaviour was observed for the other measurements of roughness (RMS and R_{max}), as shown in Table 5.

FT-IR. A comparison of FT-IR second derivative spectra, among materials based on corn starch and SEVA-C, is presented in Fig. 12.

The differences in the band at 760 cm^{-1} are associated with changes in the glucosidic ring vibration modes. The starch present on SEVA-C material withstand thermal degradation during processing, changing the functional groups associated to the glucosidic ring. Also, the bands at 860–800 cm^{-1} showed differences between

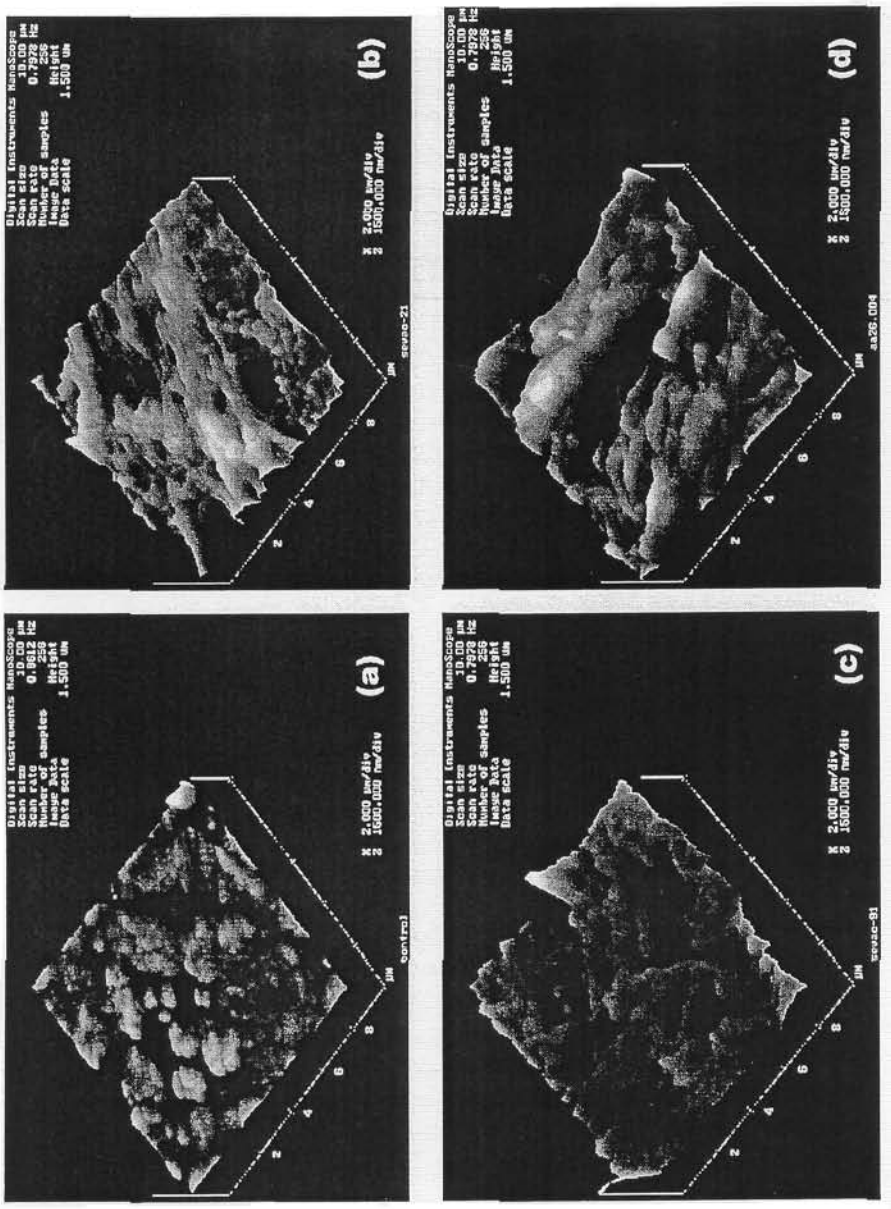

Figure 11. AFM tapping mode images. (a) Control, (b) after 21 days immersion, (c) after 91 days immersion and (d) after 101 days immersion (data scale 1500 nm and scan size 10 μm). The images present dried samples after the immersion period.

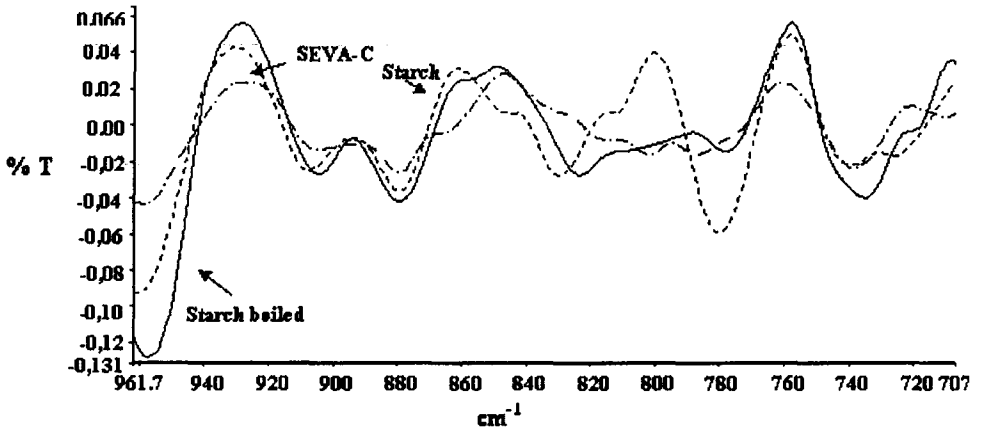

Figure 12. FT-IR second derivative spectra of SEVA-C powder before and after desegregation in boiling distilled water for 5 h.

the starch and SEVA-C; these bands might refer to the adjacent aromatic C—H patterns of the benzene ring vibration and CH_2 as a result of thermal degradation.

CONCLUSIONS

The results in this work enable us to draw the following main conclusions:

- this type of experimental studies can be carried out for relatively long periods (up to 150 days) without loss of the enzymatic activity;
- the kinetics of the degradation process depend on the enzymatic concentration for the initial period, increasing as the concentration increased in the first stages, stabilizing thereafter towards a level;
- SEM micrographs and AFM images show an increase in the surface porosity as a function of immersion time;
- the enzymatic degradation process of SEVA-C material is based on reduction of the starch macromolecules into glucose fragments, preferentially those in the amorphous phase;
- the respective degradation mechanism is based on the attack of connected starch domains, that can be accessed by the enzymatic solution; consequently, the completely encapsulated (by the EVOH) starch particles remain almost unchanged.

REFERENCES

1. M. A. Araújo, A. M. Cunha and M. Mota, *Biomaterials* **25**, 2687 (2004).
2. J. F. Mano, D. Koniarova and R. L. Reis, *J Mater Sci. Mater. Med.* **14**, 127 (2003).
3. R. L. Whistler, J. N. Bemiller and E. F. Paschall (Eds), in: *Starch Chemistry and Technology*, 2nd edn, p. 26. Academic Press, New York, NY (1984).

4. A. H. Khall, *Food Chem.* **68**, 61 (2000).
5. M. E. Gomes, P. B. Malafaya, R. L. Reis and A. M. Cunha, *Biomaterials* **22**, 883 (2001).
6. D. Dermigöz, C. Elvira, J. F. Mano, A. M. Cunha, E. Piskin and R. L. Reis, *Polym. Degrad. Stabil.* **70**, 161 (2000).
7. C. M. Vaz, A. M. Cunha and R. L. Reis, *Mater. Res. Innov.* **4**, 375 (2001).
8. S. C. Mendes, Y. P. Bovell, R. L. Reis, A. M. Cunha, J. D. Bruijn and C. A. van Blitterswijk, *Biomaterials* **22**, 2057 (2001).
9. M. E. Gomes, R. L. Reis, A. M. Cunha, C. A. van Blitterswijk and J. de Bruijn, *Biomaterials* **22**, 1911 (2001).
10. R. L. Reis and A. M. Cunha, in: *Encyclopedia of Materials Science and Technology*, p. 8910. Elsevier Science, Oxford (2001).
11. Y. Yoshida and T. Uemura, in: *Biodegradable Plastics and Polymers*. Elsevier Science, Amsterdam (1994).
12. C. Bastioli, V. Bellotti, M. Camia, L. Del Giudice and A. Rallis, in: *Biodegradable Plastics and Polymers*, p. 200, Elsevier Science, Amsterdam (1994).
13. C. Bastioli, V. Bellotti, L. Del Giudice and G. Gilli, *J. Environ. Polym. Degrad.* **1**, 181 (1993).
14. S. Simmons and E. L. Thomas, *J. Appl. Polym. Sci.* **58**, 2259 (1995).
15. R. L. Reis and A. M. Cunha, in: *ANTEC 98, Plastics on my mind*, Vol. 3, San Diego, CA, p. 165 (1998).
16. D. J. Gallant, B. Bouchet, A. Buléon and S. Pérez, *Eur. J. Clin. Nutr.* **46**, S3 (1992).
17. G. E. Zaikov, in: *Degradation and Stabilisation of Polymers*, p. 469. Elsevier Science, Amsterdam (1989).
18. E. Piskin, *Clin. Mater.* **11**, 3 (1992).
19. P. P. Klemchuck, *Polym. Degrad. Stabil.* **27**, 183 (1990).
20. G. Scott, *Polym. Degrad. Stabil.* **48**, 315 (1995).
21. E. Bailey and D. Ollis, in: *Biochemical Engineering Fundamentals*, Chapter III. McGraw-Hill, New York, NY (1986).
22. G. L. Miller, *Anal. Chem.* **31**, 426 (1959).
23. C. Van Oss C, in: *Interfacial Forces in Aqueous Media*. Marcel Dekker, New York, NY (1994).